

AN UNDERGRADUATE EXPERIMENT ON ADSORPTION

SHAMSUZZAMAN FAROOQ

National University of Singapore • Singapore 119260

Adsorption separation has become a major unit operation in the chemical process industry. Undergraduate chemical engineering students at the National University of Singapore receive about six hours of lectures on adsorption fundamentals and applications as part of the course Separation Processes II, offered in the third year of their study.

We have long felt there is a need for a suitable laboratory experiment that reinforces the basic design concepts. Since reliable equilibrium and mass transfer data are central to the design of an adsorption separation process, we have recently introduced an experiment in our third-year laboratory in which the students determine these parameters from breakthrough measurements in an adsorption column. During analysis of the breakthrough data, the students also develop a basic understanding of adsorption process dynamics.

EXPERIMENTAL APPARATUS

The experimental apparatus for breakthrough measurements, schematically shown in Figure 1, consists of a column packed with the adsorbent under study and a host of pressure and flow controllers that control the operating pressure and concentration of the adsorbate in the feed, respectively. Further details on the experimental apparatus and the adsorbent used are given in Table 1. The adsorbate is normally mixed with an inert carrier. The effluent stream is analyzed using a suitable detector to monitor the break-

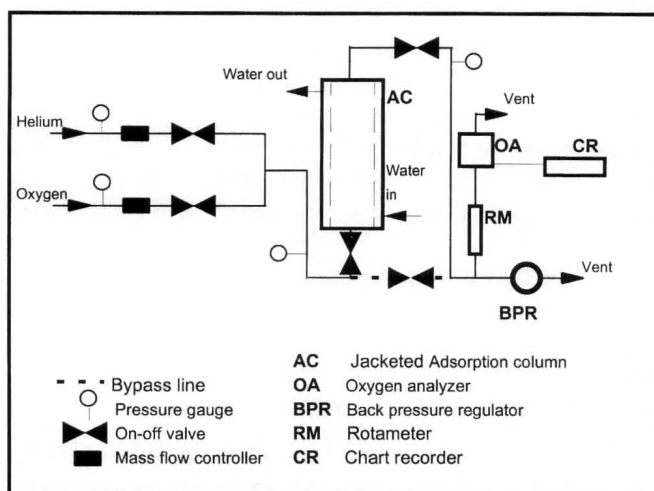


Figure 1. Schematic diagram of the breakthrough apparatus. Further details are given in Table 1.

through of the adsorbate. The desorption response is measured by withdrawing the flow of adsorbate from the feed after the column has been saturated.

THEORY

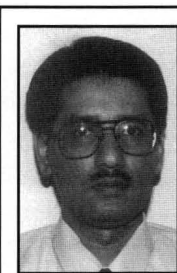
A typical breakthrough response from a clean bed to a step change in adsorbate concentration in the feed is shown in Figure 2, where c is the concentration at any time, t , and c_0 is the constant feed concentration. When the adsorbate concentration in the effluent equals that in the feed, it indicates that the bed has been saturated. Material balance over a saturated bed gives

mean residence time, \bar{t} , = (shaded area in Figure 2)

$$= \int_0^{\infty} \left(1 - \frac{c}{c_0}\right) dt = \frac{L}{v_0} \left(1 + \frac{1 - \epsilon q_0}{\epsilon c_0}\right)$$

where

- L length of packed bed
- v_0 interstitial feed velocity



Shamsuzzaman Farooq received his BSc and MSc degrees in chemical engineering from BUET (Bangladesh) and his PhD from the University of New Brunswick (Canada). A faculty member in the Chemical Engineering Department at the National University of Singapore since 1991, his research interest is in the area of adsorption gas separation. He is a coauthor of the book Pressure Swing Adsorption (VCH, 1994).

- ϵ bed voidage
- q_0 equilibrium adsorbed amount corresponding to feed concentration, c_0

A typical favorable equilibrium isotherm is shown in Figure 3. Henry's constant will be measured in this study, which requires that the experiments are conducted in the linear (low concentration) range of the isotherm. Ratio of Henry's constants of two adsorbable components is the primary measure of their separability.

It is important to note that here Henry's constant is dimensionless, since it has been expressed as concentration ratios. Henry's constant follows the Arrhenius Law of temperature dependence. The following equation is applicable for dimensionless Henry's constant:

$$K = K_0 e^{\frac{-\Delta U_0}{R_g T}}$$

where

- K_0 pre-exponential factor
- R_g gas constant in heat units
- T temperatures in absolute units

A semilogarithmic plot of K vs. $1/T$ should give a straight line with $-\Delta U_0 / R_g$ as the slope and K_0 as the intercept. The change of internal energy due to adsorption, ΔU_0 , is related

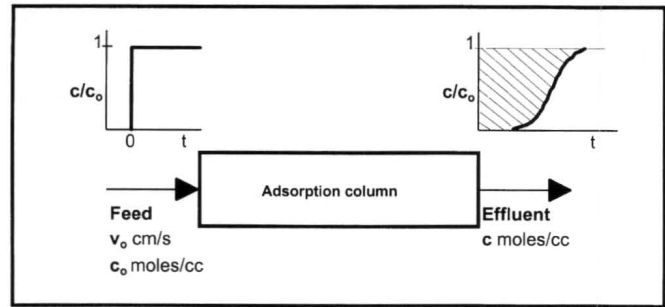


Figure 2. A typical breakthrough response for a step change in feed concentration.

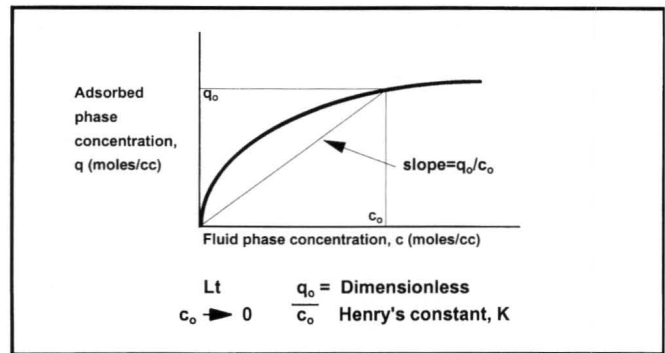


Figure 3. Favorable adsorption isotherm.

TABLE 1
Details of the Experimental Apparatus Shown in Figure 1.

<i>Item</i>	<i>Manufacturer</i>	<i>Model/Part No.</i>	<i>Range/Size</i>
Mass Flow Controllers			
• Helium line	Brooks	5850E (Controller) 0151E (display)	0-10 l/m
• Oxygen line	J & W	200-2002	built-in span adjustment from 1 cc/m to 1000 cc/m
Jacketed Adsorption Column (stainless steel)	Fabricated in the workshop		Pressure tested at 200 psi
• Length: 40 cm			
• Inner tube: 1 1/2 inch; schedule 40			
• Outer tube: 2 1/2 inch; schedule: 40			
Temperature Regulated Water Circulation	Poly Science	9101	10-95°C; 7 or 15 l/m
Oxygen Analyzer	SERVOMEX	572	Output: 0-1 V for 0-100% oxygen
Chart Recorder	Rikadenki	R-61A	100 mV full-scale setting was used
Pressure Gauge	WIKA		0-100 psi
On-Off Valves	Whitey	SS-41S2	1/8 inch
Plumbing			
• Stainless steel tube			1/8 inch
• Male connector	Swagelok	SS-200-1-2	1/8 inch
• Union	Swagelok	SS-200-6	1/8 inch
• Union elbow	Swagelok	SS-200-9	1/8 inch
Adsorbent	Carbon molecular sieve: Shirasigi MSG 3A from coconut shell. Provided by a local pharmaceutical company from the supply for their PSA nitrogen unit.		

to the limiting heat of adsorption, $\Delta U_o = \Delta H_o + R_g T$. For calculating ΔH_o from ΔU_o , the average temperature of the experimental range is used.

On the other hand, if the Henry's constant is expressed in terms of adsorbate pressure (we denote it by $K' = K/R'T$, where R' is the gas constant in pressure units), then its temperature dependence may be directly related to the heat of adsorption

$$K' = K'_o e^{\frac{-\Delta H_o}{R_g T}}$$

The desorption breakthrough is obtained when a saturated bed is purged with inert. In the linear (and very low concentration) range of the isotherm, the adsorption and desorption profiles obtained at the same velocity are symmetric.

The system of equations that describe the dynamic response of an adsorption column is given in Table 2. Analytical solution to the set of equations is given by Lapidus and Amundson^[1] in the form of complicated infinite integral. In this study, numerical solution by the method of orthogonal collocation is used. (The collocation form of the model equations may be obtained from the author upon request.) The input parameters for the model are

- Column length, $L \rightarrow$ given (40 cm)
- Bed voidage, $\epsilon \rightarrow$ given (0.35)
- Column radius, $R \rightarrow$ given (2.05 cm)
- Adsorbent particle radius, $R_p \rightarrow$ given (0.1 cm)
- Interstitial feed velocity, $v_o = u_o / \epsilon \rightarrow u_o$ is calculated from the flow rate measured during experiment (cm/s)
- Equilibrium constant, $K \rightarrow$ obtained from the breakthrough curve
- Peclet number, $Pe \rightarrow$ determined from available

correlation

- Mass transfer parameter, $k \rightarrow$ to be determined by matching the experimental breakthrough curve

$$Pe = \frac{v_o L}{D_L}$$

where $D_L = 0.7 D_m + v_o R_p$

The molecular diffusivity of the adsorbate in the carrier is D_m (cm²/s) and may be calculated from Chapman-Enskog's equation.^[2] All known commercial adsorbents offer external film, macropore, and micropore resistances to the transport of the adsorbate molecules from the bulk phase to the interior adsorption sites. A linear driving force (LDF) rate model is used here to represent the transport across these resistances, k is the overall LDF rate constant. The LDF model approximates a distributed resistance to be confined in an equivalent thin zone. The individual resistances linearly add up to give the overall LDF resistance, $1/k$:

$$\frac{1}{k} = \underbrace{\frac{R_p K}{3 k_f}}_{\text{external film resistance}} + \underbrace{\frac{R_p^2 K}{15 D_e}}_{\text{macropore resistance}} + \underbrace{\frac{r_c^2}{15 D_c}}_{\text{micropore resistance}}$$

The LDF model may be viewed as a lumped parameter model with the luxury of relating the overall constant to the more fundamental parameters that characterize the constitutive transport processes. The film mass transfer coefficient, k_f , may be calculated from the following correlation proposed by Wakao and Funazkri:^[3]

$$Sh = 2.0 + 1.1 Re^{0.6} Sc^{1/3}$$

where

Sh Sherwood number = $2 k_f R_p / D_m$

Re Reynold's number = $(2 R_p) \rho u_o / \mu$

Sc Schmidt number = $\mu / \rho D_m$

TABLE 2

Model Assumptions and Equations

(In the following equations, Y is the mole fraction of the adsorbable component in the gas phase; z is the axial distance; t is the time; P is the total system pressure; and \bar{q} is the total adsorbed amount. Other symbols are defined in the text.)

<i>Item</i>	<i>Assumptions</i>	<i>Equation</i>
Fluid phase component material balance	• Isothermal	$-D_L \frac{\partial^2 Y}{\partial z^2} + v_0 \frac{\partial Y}{\partial z} + \frac{\partial Y}{\partial t} + \frac{1-\epsilon}{\epsilon} \frac{R_g T_0}{P} \frac{\partial \bar{q}}{\partial t} = 0$
Continuity condition	• The flow pattern is described by the axial dispersed plug flow	$P \neq f(z) \neq f(t)$
Flow boundary conditions	• The frictional pressure drop is negligible • Ideal gas law holds	$D_L \left. \frac{\partial Y}{\partial z} \right _{z=0} = -v_0 \left(Y \Big _{z=0^-} - Y \Big _{z=0^+} \right); \left. \frac{\partial Y}{\partial z} \right _{z=L} = 0$
Mass transfer between fluid and particle	• The mass transfer rates are represented by linear driving force rate expressions	$\frac{\partial \bar{q}}{\partial t} = k(\bar{q}^* - \bar{q})$
Equilibrium isotherm	• Linear isotherm	$\bar{q}^* = Kc = Kc_0 Y$

ρ, μ density and viscosity, respectively.

The above correlation is particularly recommended as it was able to reconcile experimental data from a large number of sources.

$$D_e = \frac{\epsilon_p D_p}{\tau}$$

where $1/D_p = 1/D_m + 1/D_K$

The Knudson diffusivity, D_K (cm^2/s), becomes important when collision of the diffusing species with the pore walls becomes significant in comparison to the intermolecular collision. Poiseuille flow and surface diffusion are two other parallel contributions to transport in the macropores. Poiseuille flow is neglected since the pressure range in which it becomes important will not be encountered in this study.

Surface diffusion occurs through the adsorbed layer on the macropore walls. This is commonly found to be important in homogeneous adsorbents, such as activated carbon, activated alumina, silica gel, etc. For composite adsorbents, such as carbon molecular sieve and pelleted zeolites, the adsorption capacity is mainly in the micropores; the macropore walls are practically inert and the condition for surface diffusion to occur does not arise. Therefore, surface diffusion is also neglected, since we will study the adsorption and diffusion of oxygen in carbon molecular sieve. Of course, in the chosen system, both molecular and Knudson diffusion are much faster than the micropore diffusion and may be neglected as well. Nevertheless, these terms are discussed further in view of their wider conceptual importance as mechanisms of transport in porous media in general.

Knudsen diffusivity is given by

$$D_K = 9700 \xi \left(\frac{T}{M} \right)^{1/2}$$

where

ξ pore radius (cm)

T temperature (in absolute units)

M molecular weight of the adsorbate

ϵ_p, τ adsorbent particle voidage and tortuosity, respectively.

A typical value for τ / ϵ_p is approximately 10.

Therefore, in the expression for mass transfer parameter, the micropore diffusional time constant, D_c / r_c^2 , is the only unknown that is determined by matching the model solution for a breakthrough with the experimental response. Micropore diffusion is an activated process and follows Arrhenius-type temperature dependence

$$D_c = D_{c0} e^{\frac{-E}{R_g T}}$$

A semilogarithmic plot of D_c vs. $1/T$, known in the literature as the Eyring plot, will give the activation energy, E , from the slope and the pre-exponential factor, D_{c0} , as the intercept. For some adsorbents, such as carbon molecular sieve, r_c

cannot be measured explicitly. In such cases, D_c / r_c^2 is plotted against $1/T$, which yields D_{c0} / r_c^2 as an intercept.

EXPERIMENTAL PROCEDURE

The study of adsorption and diffusion of oxygen in a carbon molecular sieve is chosen as the model system here. Helium is used as the inert carrier. The following set of instructions is provided to guide the students through the various steps of the experiment.

- The oxygen analyzer response should be checked for 0 and 100% oxygen. The output range is 0-1 V and is linear. The calibration curve for the mass flow controller used for the carrier gas is provided. The total mixed flow can be easily determined by analyzing its oxygen content.
- It is suggested that the interstitial feed velocity in the column and oxygen concentration in the feed are maintained between 5 and 10 cm/s and between 2 and 4%, respectively. The adsorption column should be bypassed during flow and concentration adjustments. The system gauge pressure should not exceed 0.5 bar. The effluent is analyzed using the oxygen analyzer.
- A chart recorder is used to record the analyzer signal. The chart speed and range setting must ensure sufficient resolution of the output signal from the oxygen analyzer as a function of time.
- Water (from a temperature-regulated tank) is circulated through the jacket of the column at the desired temperature. The measurements should be conducted at three temperatures in the range of 30 to 50°C. The choice of temperatures should be evenly spaced and at least 45 minutes must be allowed for the bed to attain thermal equilibrium with the circulating water. It is also recommended to move from low to high temperature.
- The bed should be purged with helium until the 0 V baseline is attained. This ensures a clean bed with respect to oxygen.
- Introduction of the oxygen step in the feed and switching the chart on at the desired speed must occur simultaneously.
- It is essential that the breakthrough curves be measured until completion.
- It is necessary to record the desorption breakthrough curve for at least one temperature in order to check linearity of the isotherm at the chosen concentration level.
- Other than the formal desorption run, the bed is regenerated by purging with helium and increase in temperature. The adsorption breakthrough measurement is repeated when the bed has been completely regenerated and has attained the new temperature.

RESULTS AND DISCUSSION

The students are required to include the following results in their report on the experiment:

1. Plot of c/c_0 vs. time for adsorption and $(1-c/c_0)$ vs. time for desorption on the same graph in order to check the symmetry.

2. K_o , ΔU_o , and ΔH_o values from the semilogarithmic plot of K vs. $1/T$.
3. D_{co}/r_c^2 and E values from the semilogarithmic plot of D_c/r_c^2 vs. $1/T$.

Typical plots are shown in Figures 4 through 6. The parameter values determined from these plots are also shown in the respective figures. The equilibrium constant is obtained directly from the mean residence time calculated by integrating the breakthrough curves, as discussed earlier. The mass transfer parameter is obtained by matching the breakthrough profiles with the model solution. The effect of the mass transfer coefficient on the model solution is shown in Figure 7. It is clear that the model solution is quite sensitive to the value of k . The students are reminded that several numerical techniques are available to determine the best-fit values. But students carry out all the necessary computations and calculations in the laboratory and, in view of the limited laboratory time, they are allowed to use eye estimation to decide on the best fit.

While using the above method to measure D_c/r_c^2 , it is extremely important to remember that all the dispersive effects in an adsorption column (namely, axial dispersion, external film, and intraparticle diffusional resistances) that are identified in the mathematical model have similar effects on the shape of the breakthrough curve. Therefore, these effects cannot be separated from a single experiment. Moreover, since the resistances are linearly additive, there is always a risk of misinterpreting the results. Hence, there is an inherent need to always ensure that the rate parameter under investigation is indeed the controlling factor of the process dynamics. Reliable accounting of other effects is also necessary when they are not completely negligible.

Estimation of external film and macropore resistances are more reliable than prediction of axial dispersion. Maldistribution of gas flow and extra-column effects contribute to additional axial dispersion unpredictable by published correlations. Agglomeration of small particles may also result in excessive axial dispersion (see reference 3 for a comprehensive discussion). All these possibilities were taken into account while designing the experimental system used here. In order to ensure proper flow distribution, the column size was chosen to satisfy the recommended column-to-particle diameter ratio. Furthermore, 1/8-inch tubes and fitting were used to minimize extra-column mixing effects. In spite of all these precautions, experimental verification is recommended to confirm that the associated dispersive effects are correctly estimated.

Although the available laboratory time is not sufficient to include such supporting experiments, the students do not remain ignorant on these matters. In addition to writing a general discussion on the findings, they are also asked to suggest an experiment to prove that the present system is micropore-diffusion controlled and to comment on the effect

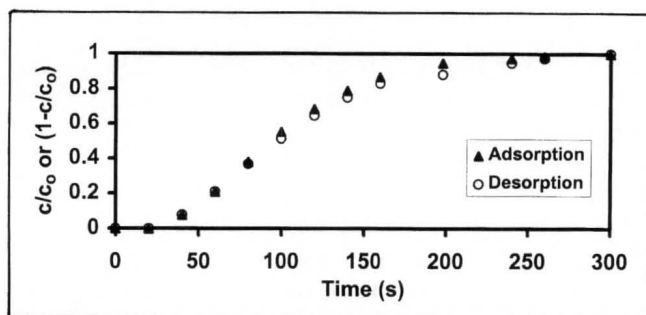


Figure 4. Symmetry of the adsorption and desorption breakthrough curves in the linear range of the equilibrium isotherm.

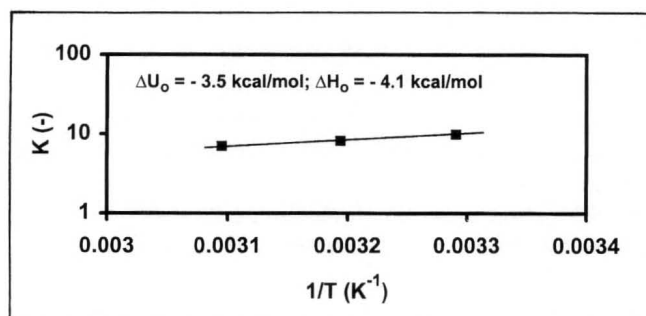


Figure 5. Temperature dependence of Henry's constant (oxygen in a carbon molecular sieve) showing that it follows Arrhenius Law.

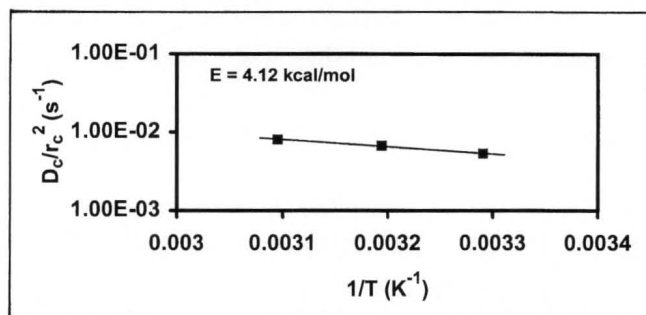


Figure 6. Eyring plot showing temperature dependence of micropore diffusivity for the diffusion of oxygen in a carbon molecular sieve.

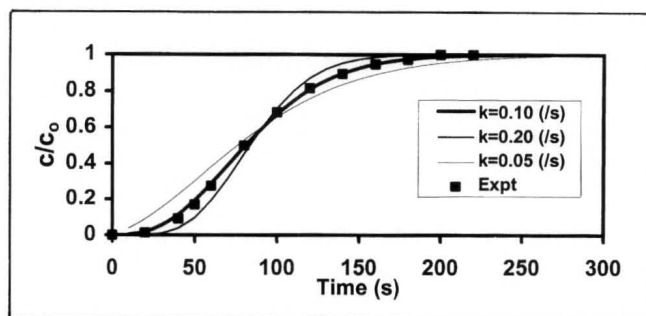


Figure 7. Effect of LDF mass transfer coefficient (k) on the model solution.

of macropore size and operating pressure on the macropore resistance. These questions guide their thoughts to the following important points:

- For a micropore-controlled system, a reduction in the macroparticle size should not affect the mass transfer kinetics. Hence, when the k value remains unaffected by a change in the particle size, it serves as clear proof that the axial dispersion and macropore resistance are practically negligible. On the other hand, a variation in values estimated from experimental runs with different particle size and/or at different velocities will indicate that the secondary resistances are not negligible and their contributions have not been properly estimated.
- The importance of Knudsen diffusivity depends on the effective macropore size and is independent of pressure, whereas molecular diffusivity is inversely proportional to pressure and may affect the overall transport rate at a higher pressure.

CONCLUSIONS

This laboratory exercise introduces the students to the calculations of equilibrium and kinetic parameters for an adsorption separation process. The use of a dynamic model for the extraction of the mass transfer parameter provides a useful visualization of the role of this parameter on process performance. The simulation model can also be effectively used to illustrate in detail the numerical solution of a system of coupled partial differential equations. The consistency of results obtained by different groups is encouraging. Equilibrium capacity and mass transfer resistance of the chosen system are well suited for completing the required number of runs and necessary computations in one standard laboratory session of six hours.

REFERENCES

1. Lapidus, L., and N.R. Amundson, *J. of Phy. Chem.*, **56**, 984 (1952)
 2. Sherwood, T.K., R.L. Pigford, and C.R. Wilke, *Mass Transfer*, McGraw-Hill, New York, NY; Chap. 2
 3. Ruthven, D.M., *Principles of Adsorption and Adsorption Processes*, Wiley Interscience, New York, NY, Chap. 7 (1984)
-

BOOK REVIEW: *Batch Distillation*

Continued from page 13.

Example 1.2 are easily misinterpreted. And there is a technical mistake in the calculation of the heat to the reboiler in Eqs. (2.13) and (2.17). The author ignores the energy required to vaporize the distillate product in the reboiler. Equation 2.13 should be $Q_R = \lambda(R+1)D$.

The graduate-level material starts in Chapter 3, "Column Dynamics," which derives the unsteady mass and energy balances. Then error, stability, and a summary of numerical integration techniques are presented. The need for an integration technique capable of handling stiff equations is clearly illustrated in Example 3.1. The chapter is completed

Winter 1998

with sections on start-up and approximate models. There are some parts that will confuse students. For example, the numbering of stages in Figure 3.1 does not agree with the equations, and derivation of Eq. (3.44) requires assumptions not mentioned in the text.

The author is clearly an expert on the application of shortcut (Fenske-Underwood-Gilliland) methods to batch distillation. Readers are told to "be careful in choosing the appropriate value for the light key and heavy key for successful use of this method," but how to be careful is not explained. This and other small mysteries will cause confusion. The modified shortcut method developed next requires lumping a number of plates into compartments. Other than comparison with an exact solution, no guidance is given on how to select the number of plates in each compartment. The last section on the hierarchy of models in the simulator will be very helpful to students using the simulator.

Chapter 5, "Optimization," describes objective functions, degree of freedom analysis, feasibility, and the general framework of solution methods. This chapter is quite general and would benefit greatly from numerical examples. Chapter 6 on optimal control problems builds on Chapter 5. This chapter would also benefit from numerical examples in addition to the derivation examples.

The last chapter analyzes azeotropic systems and columns with a middle vessel. Since most students will be unfamiliar with the analysis of steady state azeotropic distillation, more details on residue curve maps and synthesis of batch distillation systems would be welcome. The shortcut method is extended to binary azeotropic systems and simple ternary systems. Extension to more complicated ternary azeotropic systems would be welcome.

The index appears to be quite well done. An author index would be appreciated. The reference lists at the end of each chapter appear to include all the important historical and recent papers. The nomenclature list is quite complete, and the tables that summarize the equations after each theoretical development are helpful. The type is easy to read and there appear to be few typographical errors. Unfortunately, the figures are not of professional quality and are difficult to interpret. Many of the figures have multiple curves that are not labeled. When two theories are compared on the same figure, the reader needs to guess which is which. The curves are not smooth and it is often unclear if the wiggles are real or due to the plotting routine.

Every chemical engineering department should obtain a copy for their library's reserve section. Chapters 1 and 2 will be helpful as a reference for undergraduates doing laboratory or design projects on binary batch distillation. The remainder of the book will help graduate students and professors who occasionally encounter multicomponent batch distillation problems. □

81